Received: 19 October 2021 | Accepted: 8 August 2022

DOI: 10.1002/hep4.2074

ORIGINAL ARTICLE

Dysregulation of global circular RNA abundance regulated by spliceosomes predicts prognosis in hepatocellular carcinoma

Lei He[1,2] | **Liman Qiu**[1] | **Feng Chen**[1] | **Tingting Chen**[1] | **Fang Peng**[1,2] | **Zhenli Li**[1] | **Xiuqing Dong**[1] | **Zhixiong Cai**[1] | **Yuanchang Fang**[1] | **Hengkai Chen**[1] | **Geng Chen**[1] | **Xiaolong Liu**[1]

[1]The United Innovation of Mengchao Hepatobiliary Technology Key Laboratory of Fujian Province, Mengchao Hepatobiliary Hospital of Fujian Medical University, Fuzhou, P. R. China

[2]Mengchao Med-X Center, Fuzhou University, Fuzhou, P. R. China

Correspondence
Geng Chen and Xiaolong Liu, The United Innovation of Mengchao Hepatobiliary Technology Key Laboratory of Fujian Province, Mengchao Hepatobiliary Hospital of Fujian Medical University, Xihong Road 312, Fuzhou 350025, Fujian Province, P. R. China.
Email: thestaroceanster@hotmail.com and xiaoloong.liu@gmail.com

Funding information
National Natural Science Foundation of China, Grant/Award Number: 81802413; Scientific Foundation of Fujian Province, Grant/Award Number: 2019J01139

Abstract

CircRNAs have been reported to play crucial roles in tumor progression and recurrence, showing potential as biomarkers in cancer. However, the global abundance of circRNA and their involvement in hepatocellular carcinoma (HCC) development have not been fully explored. Whole transcriptome sequencing was performed on tumor and peritumor from 60 patients with HCC to quantify the expression of circRNAs, and the global circRNA abundance was calculated by circRNA index (CRI). Gene-set enrichment analysis and weighted gene co-expression network analysis were used to reveal the biological signaling pathways associated with the global circRNA abundance. The correlation between the global circRNA abundance and the infiltration level of $CD8^+$ T cells was explored by immunohistochemical assays. Small interfering RNA was used to knock down the pre–messenger RNA spliceosome in HCC cell lines to verify the regulation of spliceosome in global circRNA abundance. We found that dysregulation of global circRNA abundance in both tumor and peritumor could lead to worse prognosis. The immunohistochemical assay further revealed that the dysregulation of global circRNA abundance in both tumor and peritumor would obstruct the $CD8^+$ T cells from invading into the tumor, which might explain its correlation with HCC prognosis. We also demonstrated that the spliceosome genes were the main factors to regulate the global circRNA abundance in HCC, and these results were also confirmed by knockdown experiments. *Conclusion*: This study revealed the association between the global circRNA abundance and patients' prognosis and its underlying mechanism.

Lei He and Liman Qiu contributed equally to this work.

INTRODUCTION

As the most common primary liver cancer, HCC is a deadly malignancy with rapidly increasing morbidity and mortality.[1] Like many other cancer types, one key characteristic of HCC is its abnormal gene expression, which is considered to be one of the essential conditions for tumorigenesis and progression.[2] Being a key component of transcriptome, circular RNAs (circRNAs) could participate in multiple physiological processes, including blocking the inhibitory effects of microRNAs on target genes,[3,4] binding to RNA-binding proteins to regulate the expression of specific genes,[5,6] even encoding short peptides with specific functions,[7] all of which are reported to be associated with HCC development. Because of the closed-loop structure, circRNAs are more stable than linear RNAs and therefore possess great potential as tumor biomarkers and clinical therapeutic targets in HCC.[8] Although many studies have dedicated their efforts to discover the relationship between specific circRNAs and tumor progression, the landscape of global circRNA abundance as a whole in HCC is still poorly investigated. Our and other previous studies have shown that circRNA levels in tumors were almost always lower than peritumors,[9,10] suggesting consistent trends of reducing circRNA abundance during tumorigenesis, which indicate the potential correlation between global circRNA abundance and tumor status. Thus, the global abundance of circRNAs, which presented an integrated view for the transcriptome, might provide a better evaluation for the disease status of patients with cancer. Interestingly, a recent study has reported that global circRNA abundance could serve as an indicator for clinically relevant subtypes in prostate tumors, whereas patients with circRNA abundance more deviate from the median value showed worse prognosis, indicating that the dysregulation of global circRNA abundance is closely related with tumor progression.[11] However, the biological mechanism of this relation still remained largely unknown. Furthermore, as a highly heterogenous tumor, the transcriptome of HCC is also highly heterogenous; therefore, how global circRNA abundance affected HCC prognosis still needs further exploration.

A noteworthy fact is that HCC is considered to be the product of long-term co-evolution between cancer cells and their environmental components,[12–18] which mostly occurs in the inflammatory microenvironment of hepatitis and cirrhosis.[19] Thus, the peritumor of HCC not only provides the soil for tumorigenesis, but also compromises the inflammatory microenvironment that is essential for tumor progression. Serving as an outline boundary where tumor and microenvironment interact, the transcriptome of peritumor in HCC might also play some role in tumor progression and thus might provide valuable insight into patients' prognosis. However, this territory is poorly investigated, and an evaluation of peritumor circRNA landscape might help to illustrate its significance.

One major factor influencing global circRNA abundance is its biogenesis, which involved two mechanisms: direct back-splicing and exon skipping,[20] in which the generation of most circRNAs is considered as alternative splicing events with almost the same small nuclear RNA and splice factor components involved as corresponding canonical splicing events.[21] Liang et al. revealed that inhibition of the spliceosome could markedly increase the ratio of circular to linear RNAs.[22] A similar phenomenon was also reported in mouse.[23] These studies hinted that the spliceosome might play a part in the dysregulation of global circRNA abundance, however, whether such regulation mechanism exists in HCC still needs further investigation.

To fully evaluate the global circRNA abundance in HCC and reveal its significance in patients' prognosis, we performed strand-specific and ribosomal RNA-depleted RNA-sequencing (RNA-seq) on tumors and paired peritumors collected from 60 patients with HCC. We discovered that global circRNA abundance in both tumor and peritumor could indeed serve as an indicator for HCC prognosis, with its dysregulation leading to worse survival. Meanwhile, we also found that the global circRNA abundance was regulated by pre–messenger RNA (mRNA) splicing factors in mechanism. Taking together, our data show that the pre-mRNA splicing factor misregulation could lead to global circRNA abundance dysregulation in tumor, and then deviated global circRNA abundance could further accelerate tumor progression.

METHODS

Clinical samples

A total of 60 patients with HCC who received surgical operation at Mengchao Hepatobiliary Hospital of Fujian Medical University were enrolled. During surgery, their primary tumor samples and matched peritumor samples were collected and fresh-frozen for downstream analysis. The study design and human sample use were approved by the Ethics Committee of Mengchao Hepatobiliary Hospital of Fujian Medical University (approval ID of 2017_023_01), and written informed consent was obtained from all patients. The methodology conformed to the standards set out in the Helsinki Declaration.

Cell culture

Human HCC cell line SK-Hep-1 was purchased from the Chinese Cell Bank of the Chinese Academy of Sciences (Shanghai, China). This human cell line has

been authenticated using single-nucleotide polymorphism profiling. Cells were cultured in Dulbecco's modified Eagle medium (Gibco) with 10% fetal bovine serum (ExCell Bio) under an atmosphere of 95% humidified air and 5% CO_2 at 37°C. All experiments were performed with mycoplasma-free cells.

Tissue and cell-line RNA-seq

The total RNA of tissues collected during surgery and cell lines was extracted with TransZol Up Plus RNA Kit (TransGen Biotech) according to manufacturer's instructions. RNA samples underwent quality control with capillary electrophoresis. For each sample, 1 μg of total RNA was used for ribosomal RNA (rRNA) removal with the Ribo-off rRNA Depletion Kit (Human/Mouse/Rat), and then subject to library preparation for RNA-seq using the VAHTS Universal V8 RNA-seq Library Prep Kit for Illumina according to the manufacturer's instructions. The quality and yield after sample preparation were measured with the capillary electrophoresis (Qsep 100 Bioptic). RNA-seq libraries were sequenced as 150-bp paired-end reads using NovaSeq platforms.

Immunohistochemistry

Immunohistochemistry (IHC) staining was performed at Wuhan Servicebio Technology. Human anti-CD8 Rabbit pAb (GB13068; Servicebio) was used to assess $CD8^+$ infiltrating T cells on 4-μm-thick formalin-fixed paraffin-embedded tumor tissue slides. Images were captured with OCUS portable digital scanning microscopic imaging system (APG Bio). After a quick examination of slide quality, the images were imported into the ImageJ software (National Institutes of Health), and the positive areas were calculated as infiltration level.

Real-time quantitative polymerase chain reaction

Total RNA was extracted from SK-Hep-1 cells with Trizol reagent (TransGen Biotech), and reverse transcription was carried out using the Transcriptor First Strand cDNA Synthesis Kit (Roche). Specific primers of sizes ranging from 20–25 bp (Table S2) were designed to detect pre-mRNA spliceosome genes. Expression levels of pre-mRNA spliceosome genes were quantified using the SYBR Premix Ex Taq II (Takara) in StepOne Software V2.3 thermal circulation system. The amplification parameters were set as follows: predenaturation at 95°C for 10 min, denaturation at 95°C for 30 s, annealing at 60°C for 30 s, extension at 72°C for 30 s, for a total of 40 cycles. 18S was used as the endogenous control gene. Quantification of quantitative real-time polymerase chain reaction (PCR) was calculated by the $2^{-\Delta\Delta Ct}$ method.

Transfection and expression suppression

All small interfering RNA (siRNA) sequences used in this study are listed in Table S3. The siRNA was transfered to SK-Hep-1 cells by Lipofectamine 3000. A total of 3×10^5 cells were plated in 6-well plates overnight and transfected the next day with the transfection mixture (6 μl lipofectamine 3000 and 15 μl 20 μm siRNAs in 250 μl Opti-MEM I Reduced Serum Medium) for 48 h before cell collection and downstream experiments.

RNA-seq data processing

To measure the expression level of mRNAs, RNA-seq reads were mapped to GRCh37 with Gencode v24lift37 annotation[24] using STAR (v2.7.4).[25] Then, the resulting bam file from STAR was used as input to the rsem-calculate-expression program (v1.3.1).[26]

CircRNA identification and quantification of circRNA overall abundance

CircRNAs were identified by CIRI2 (v2.0.4)[27] with the RNA-seq sequencing data, using GRCh37 reference and Gencode (v24lift37) annotations. circRNAs identified in each sample were merged together, and the numbers of back-splicing reads were extracted to measure their abundance. Only circRNAs with more than two back-splicing junction reads (reads encompassing back-splicing site) in at least half of 60 paired HCC tissue samples and matched peritumor tissue samples were kept for downstream analysis. The number of junction reads was used as quantification value in the downstream analysis. To quantify the overall abundance of circRNA expression, we used the circRNA index (CRI) from Chen's research,[11] which was defined as the number of circRNAs that showed abundance higher than the mean value across certain category of samples.

Univariate survival analysis

Univariate survival analysis was performed on global circRNA abundance using the Kaplan–Meier. Assumption for the Cox proportional hazards models was tested using the coxph function in the R Survival package (v3.2-3) (Therneau and Grambsch, 2013) with 0.05 as *p* value cutoff. Data visualization was performed using the R package survminer (v0.4.8).

Gene-set enrichment analysis

Differential expression analysis was performed between the Extreme and Stable groups using R package limma (v3.40.6),[28] and then gene-set enrichment analysis (GSEA) was performed using the R package clusterprofiler.[29] The c2.cp.kegg.v7.2.entrez.gmt and c5.go.bp.v7.2.entrez.gmt were used for GSEA.

Weighted correlation network analysis and GSEA

To get the gene sets that associated with global circRNA abundance, the expression of genes (median absolute deviation >1) was collected as input to weight the weighted gene co-expression network analysis (WGCNA).[30] Then, GSEA was performed with R package clusterprofiler (v3.14.3)[29] on the gene modules related to CRI. The false discovery rate method was used for multiple hypotheses testing correction (correction_method = FDR).

Statistical analysis

The comparison of $CD8^+$ T-cell infiltration level between different sample groups was conducted using Wilcoxon signed-rank test. Dunnett t-test was deployed to investigate the significance of differences for spliceosome gene expression quantified by quantitative PCR between control and corresponding knock-down groups. The comparison of proliferation and migration ability inferred by CCK8 and wound-healing assay between control and knock-down groups was conducted using unpaired *t* tests. *p* Values less than 0.05 were considered statistically significant.

RESULTS

Dysregulation in global circRNA abundance indicates worse prognosis of HCC

To assess the expression landscape of circRNAs in HCC, 60 patients with HCC receiving surgical operation at Mengchao Hepatobiliary Hospital of Fujian Medical University were enrolled from 2014 to 2019. Enrolled patients had a mean tumor size of 6.81 cm (1–22 cm, in whom 56.7% had vascular invasion and 16.7% had multiple tumors; Table 1). Paired HCC tumor and peritumor tissues were collected during surgery and subjected to strand-specific and rRNA-depleted RNA-seq. After sequencing data processing, we first performed CIRI2 to identify circRNAs. A total of 43,980 circRNAs were fully rebuilt with at least two back splice junction reads in one sample. To provide a quantitative measure of global circRNA abundance, we adopted the CRI from Chen's study.[11] For each type of tissue samples (i.e., tumor or peritumor), the CRI for each sample is defined as the number of circRNAs showing expression higher than the mean expression across all samples of the corresponding type. Thus, higher CRI indicated relatively higher global circRNA abundance. Considering the stable characteristics of circRNAs, the global circRNA abundance should generally be at a relatively stable level, while perturbation of the global abundance might affect tumor progression. Based on this hypothesis, we divided patients according to their deviation away from the median CRI, and further explored the effect of global circRNA abundance fluctuations on HCC progression.

According to their CRI expression pattern in tumor, patients with HCC could be divided into quantiles, with the upper quantile (G4, n = 17) and lower quantile (G1, n = 14) grouped as the tumor-extreme ($T_{extreme}$) group and the other two quantiles (G2, n = 13; G3, n = 16) grouped as the tumor-stable (T_{stable}) group (Figure 1A). Similar division could be performed separately based on CRI in peritumor samples, resulting in the peritumor-extreme ($P_{extreme}$; G4, n = 15; G1, n = 15) group and the peritumor-stable (P_{stable}; G2, n = 14; G3, n = 16; Figure 1D). The results showed that patients in the $T_{extreme}$ group have significantly shorter overall survival (OS) and recurrence-free survival (RFS) compared with the T_{stable} groups (Figure 1B,C; $p = 0.033$ for OS, $p = 0.019$ for RFS), which is consistent with the study in prostate tumors.[11] Meanwhile, patients in the $P_{extreme}$ group also have worse prognosis compared with the P_{stable} group (Figure 1E,F; $p = 0.0011$ for OS, $p = 0.13$ for RFS). Furthermore, multivariate Cox analysis showed that CRI in both tumor and peritumor could serve as an independent risk factor for HCC prognosis (Figure 1G,H; $p = 0.01195$ in tumor for OS and $p = 0.01025$ in peritumor for OS).

Comparing the patients' clinical characteristics in different CRI-based groups, we found that patients with multiple tumors (≥2) were more likely to be classified as the $T_{extreme}$ group ($p = 0.008$; Figure S1C; Table 1), which means they tend to show dysregulation of global circRNA abundance. Meanwhile dysregulation of global circRNA abundance of peritumor was significantly related with tumor size and microvascular invasion, with the $P_{extreme}$ group having significantly larger tumor ($p = 0.0001$; Figure S1A) and more severe microvascular invasion ($p = 0.0371$; Figure S1B; Table 2). These results revealed that dysregulation circRNA abundance in tumor or peritumor both indicated poor prognosis for HCC and might be related to different clinical parameters.

As tumor and peritumor both contributing to the progression of HCC, a categorization using both tumor and peritumor global circRNA abundance might further

TABLE 1 Correlation of the clinicopathological characteristics with tumor circRNA abundance in HCC

	Tumor-stable (n = 29)	Tumor-extreme (n = 31)	Overall (n = 60)	*p* Value
Age (years)				0.438323
<55	13 (44.8%)	17 (54.8%)	30 (50.0%)	
≥55	16 (55.2%)	14 (45.2%)	30 (50.0%)	
Height (m)				0.08737
Mean (±SD)	1.69 (±0.0737)	1.68 (±0.0545)	1.69 (±0.0639)	
Weight (kg)				0.087273
Mean (±SD)	63.2 (±8.19)	67.6 (±10.3)	65.5 (±9.54)	
Gender				0.3744
Male	23 (79.3%)	29 (93.5%)	52 (86.7%)	
Female	6 (20.7%)	2 (6.5%)	8 (13.3%)	
Smoke				0.127978
Never	23 (79.3%)	19 (61.3%)	42 (70.0%)	
Ever	6 (20.7%)	12 (38.7%)	18 (30.0%)	
Alcohol				0.280546
Never	24 (82.8%)	22 (71.0%)	46 (76.7%)	
Ever	5 (17.2%)	9 (29.0%)	14 (23.3%)	
AFP				0.3662
>20	13 (44.8%)	18 (58.1%)	31 (51.7%)	
≤20	15 (51.7%)	13 (41.9%)	28 (46.7%)	
Not reported	1 (3.4%)	0 (0%)	1 (1.7%)	
HBV				0.18957
Negative	18 (62.1%)	14 (45.2%)	32 (53.3%)	
Positive	11 (37.9%)	17 (54.8%)	28 (46.7%)	
Tumor number**				**0.007877**
Solitary	**28 (96.6%)**	**22 (71.0%)**	**50 (83.3%)**	
Multiple (≥2)	**1 (3.4%)**	**9 (29.0%)**	**10 (16.7%)**	
Tumor size				0.221118
Mean (±SD)	6.90 (±4.25)	6.72 (±4.90)	6.81 (±4.56)	
Differentiation				0.767669
Mild	17 (58.6%)	17 (54.8%)	34 (56.7%)	
Severe	12 (41.4%)	14 (45.2%)	26 (43.3%)	
Vascular invasion				0.45491
No	14 (48.3%)	12 (38.7%)	26 (43.3%)	
Yes	15 (51.7%)	19 (61.3%)	34 (56.7%)	
Tumor encapsulation				0.2828
None	21 (72.4%)	24 (77.4%)	45 (75.0%)	
Complete	8 (27.6%)	5 (16.1%)	13 (21.7%)	
Not reported	0 (0%)	2 (6.5%)	2 (3.3%)	
BCLC				0.244217
A	21 (72.4%)	18 (58.1%)	39 (65.0%)	
B + C	8 (27.6%)	13 (41.9%)	21 (35.0%)	
TNM				1
I–II	20 (69.0%)	20 (64.5%)	40 (66.7%)	
III–IV	9 (31.0%)	10 (32.3%)	19 (31.7%)	
Not reported	0 (0%)	1 (3.2%)	1 (1.7%)	

TABLE 1 (Continued)

	Tumor-stable (n = 29)	Tumor-extreme (n = 31)	Overall (n = 60)	*p* Value
MVI				0.276088
M0	11 (37.9%)	5 (16.1%)	16 (26.7%)	
M1	2 (6.9%)	2 (6.5%)	4 (6.7%)	
M2	4 (13.8%)	7 (22.6%)	11 (18.3%)	
Not reported	12 (41.4%)	17 (54.8%)	29 (48.3%)	

Note: Bold text with "*" represents *p* values with significant difference (*$p<0.05$, **$p<0.01$, ***$p<0.001$).
Abbreviations: BCLC, Barcelona Clinic Liver Cancer; MVI, microvascular invasion; TNM, tumor node metastasis.

improve the prognosis prediction of patients with HCC. As expected, among 60 enrolled patients, patients with extreme global circRNA abundance in both tumor and peritumor, which were grouped as E–E (n = 18), showed worst prognosis, whereas patients with stable global circRNA abundance in both tumor and peritumor, which was grouped as S-S (n = 17), showed the best prognosis and had the longest OS and RFS (Figure S1D,E; $p = 0.001$ for OS; $p = 0.023$ for RFS). The results indicate a strategy for evaluating HCC prognosis based on the global circRNA abundance.

Functional characterization of the global circRNA abundance in HCC

To determine how dysregulation of global circRNA abundance promotes HCC progression, we performed GSEA and WGCNA to explore the functional characterization related to global circRNA abundance. GSEA analysis revealed that the $T_{extreme}$ group was primarily enriched with the gene signatures related to tumor growth and tumor immunoreaction such as "signaling pathways regulating pluripotency of stem cells," "Wnt signaling pathway," and "TGF-beta signaling pathway" (Figure 2A), which was consistent with the prognostic result. Meanwhile, WGCNA analysis based on global circRNA abundance in tumor identified a gene module related to CRI (MEgreen, $p = 0.01$), including well-known HCC-related genes such as CXCL13,[31] FAM122C,[32] and CELF2.[33] Furthermore, Gene Ontology and Kyoto Encyclopedia of Genes and Genomes analysis of the module showed that genes were significantly enriched in immune regulatory pathways, indicating a potential relationship between global circRNA abundance and immune regulation (Figure 2C). Similar analysis in peritumor revealed a significant correlation between global circRNA abundance and immunomodulatory (Figure 2B), and inflammatory factor-related pathways contained genes of the human antibody heavy chain gene family, which were reported to be involved in the regulation of immune cell activation.[34] Meanwhile, the WGCNA analysis showed that the gene sets associated with global circRNA abundance (MEturquoise, $p = 0.01$) were significantly enriched in pathways of regulating mRNA formation (Figure 2D), which indicated that formation of circRNAs was likely to be also affected by regulators of their mRNA counterpart.

Collectively, these results further verified that dysregulation circRNAs in HCC might promote the biological processes associated with tumor growth and create an immunosuppressive tumor microenvironment in patients with HCC. A potential ripple effect may happen in the tumorigenesis of HCC, that the global circRNA abundance was regulated by pre-mRNA spliceosome, and then the fluctuation of global circRNA abundance may promote HCC progression by immune-related pathways in both tumor and peritumor.

Connection between the dysregulation of global circRNA abundance and immune infiltration

As aforementioned results, the global circRNA abundance in both tumor and peritumor is closely correlated with T-cell regulation-related pathways, including T-cell activation and T helper differentiation, suggesting their connection to immune response. $CD8^+$ T cells (i.e., cytotoxic T cells) have been reported to play crucial roles in defense against tumor, and their infiltration level in tissues is often considered as a reliable quantification measurement of immune response. Thus, we detected the infiltration level of $CD8^+$ T cells in HCC paraffin section through IHC analysis to evaluate their immune infiltration level. Among the enrolled 60 patients, 21 of them had histologic sections available, with 12 having both tumor and peritumor tissue sections. These patients were thus selected for downstream IHC experiments to determine the level of $CD8^+$ T-cell infiltration. The results showed that $CD8^+$ T-cell infiltration level in tumor tissue for the $T_{extreme}$ group was significantly lower than the T_{stable} group (Figure 3A,B), indicating that the immune infiltration is notably scarce in the $T_{extreme}$ group. Meanwhile, the IHC results of

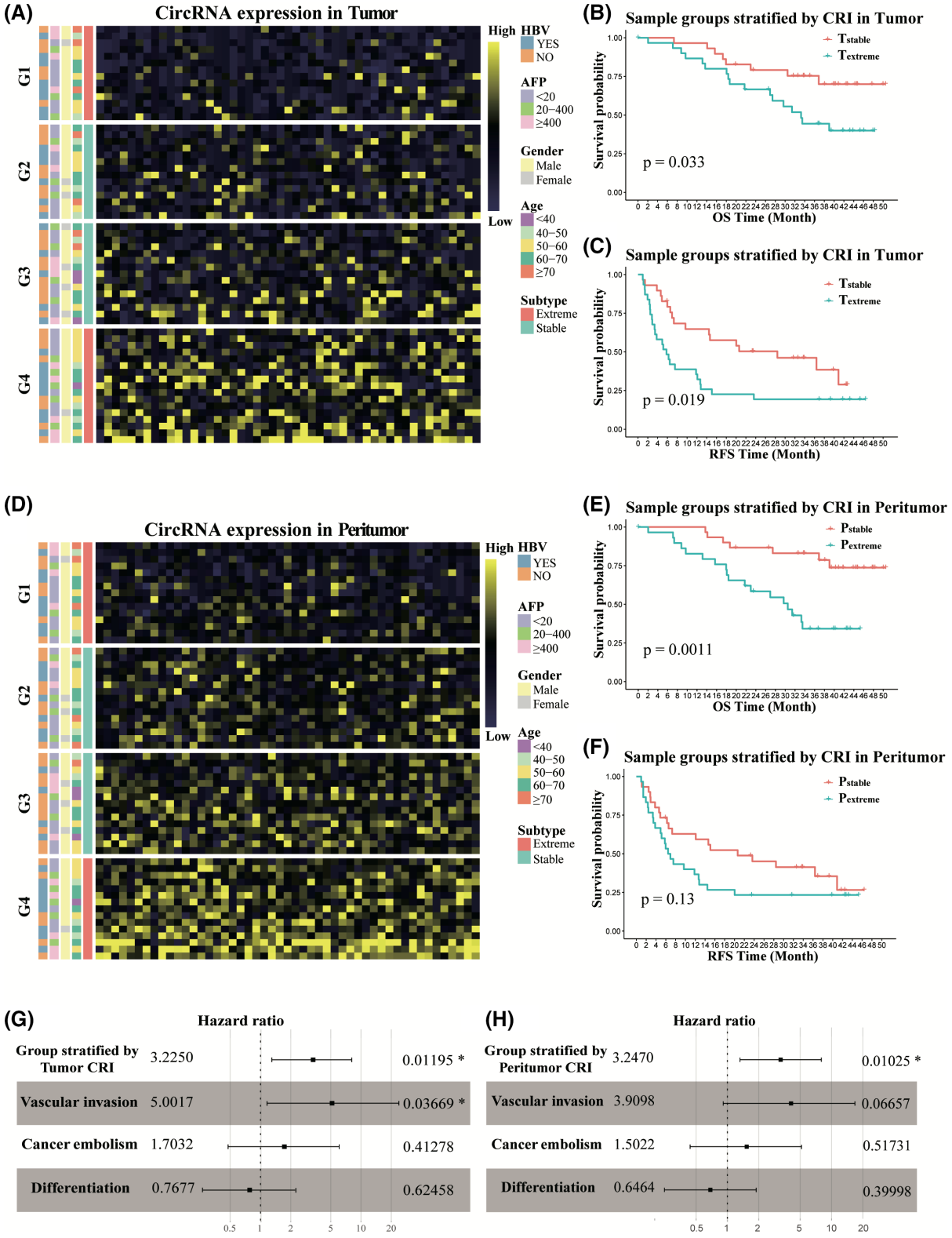

FIGURE 1 Dysregulation of circular RNAs (circRNAs) in tumor and matched peritumor is associated with hepatocellular carcinoma (HCC) progression. (A) Relative global circRNA abundance across 60 HCC tumors, represented by circRNA expression. Patients were ranked according to the increasing of circRNA index (CRI) and divided into quartile groups (G1–G4). (B,C) Comparison of overall survival and recurrence-free survival between the T_{stable} (G2, G3) and $T_{extreme}$ (G1, G4) groups. (D) Relative global circRNA abundance across 60 peritumors, represented by circRNA expression. Patients were ranked according to the increasing of CRI and divided into quartile groups (G1–G4). (E,F) Comparison of overall survival and recurrence-free survival between the P_{stable} (G2, G3) and $P_{extreme}$ (G1, G4) groups. (G,H) Group categorization based on tumor and peritumor CRI are both independent risk factors for HCC overall survival. AFP, alpha-fetoprotein; HBV, hepatitis B virus; OS, overall survival; RFS, recurrence-free survival.

TABLE 2 Correlation of the clinicopathological characteristics with peritumor circRNA abundance in HCC

	Peritumor-stable (n = 30)	Peritumor-extreme (n = 30)	Overall (n = 60)	*p* value
Age (years)				0.121335
<55	12 (40.0%)	18 (60.0%)	30 (50.0%)	
≥55	18 (60.0%)	12 (40.0%)	30 (50.0%)	
Height (m)				0.493744
Mean (±SD)	1.69 (±0.0682)	1.68 (±0.0603)	1.69 (±0.0639)	
Weight (kg)				0.313177
Mean (±SD)	64.1 (±8.99)	66.9 (±10.0)	65.5 (±9.54)	
Gender				0.706469
Male	25 (83.3%)	27 (90.0%)	52 (86.7%)	
Female	5 (16.7%)	3 (10.0%)	8 (13.3%)	
Smoke				0.573138
Never	20 (66.7%)	22 (73.3%)	42 (70.0%)	
Ever	10 (33.3%)	8 (26.7%)	18 (30.0%)	
Alcohol				0.541552
Never	22 (73.3%)	24 (80.0%)	46 (76.7%)	
Ever	8 (26.7%)	6 (20.0%)	14 (23.3%)	
AFP				0.1984
>20	13 (43.3%)	18 (60.0%)	31 (51.7%)	
≤20	17 (56.7%)	11 (36.7%)	28 (46.7%)	
Not reported	0 (0%)	1 (3.3%)	1 (1.7%)	
HBV				0.300623
Negative	18 (60.0%)	14 (46.7%)	32 (53.3%)	
Positive	12 (40.0%)	16 (53.3%)	28 (46.7%)	
Tumor number				0.488422
Solitary	24 (80.0%)	26 (86.7%)	50 (83.3%)	
Multiple (≥2)	6 (20.0%)	4 (13.3%)	10 (16.7%)	
Tumor size***				**0.000111**
Mean (±SD)	**5.04 (±2.46)**	**8.58 (±5.46)**	**6.81 (±4.56)**	
Differentiation				0.297365
Mild	15 (50.0%)	19 (63.3%)	34 (56.7%)	
Severe	15 (50.0%)	11 (36.7%)	26 (43.3%)	
Vascular invasion*				**0.037142**
No	**17 (56.7%)**	**9 (30.0%)**	**26 (43.3%)**	
Yes	**13 (43.3%)**	**21 (70.0%)**	**34 (56.7%)**	
Tumor encapsulation				0.7627
None	21 (70.0%)	24 (80.0%)	45 (75.0%)	
Complete	8 (26.7%)	5 (16.7%)	13 (21.7%)	
Not reported	1 (3.3%)	1 (3.3%)	2 (3.3%)	
BCLC				0.17595
A	22 (73.3%)	17 (56.7%)	39 (65.0%)	
B + C	8 (26.7%)	13 (43.3%)	21 (35.0%)	
TNM				0.1769
I–II	23 (76.7%)	17 (56.7%)	40 (66.7%)	
III–IV	7 (23.3%)	12 (40.0%)	19 (31.7%)	
Not reported	0 (0%)	1 (3.3%)	1 (1.7%)	

(Continues)

TABLE 2 (Continued)

	Peritumor-stable (n = 30)	Peritumor-extreme (n = 30)	Overall (n = 60)	*p* value
MVI				0.723
M0	8 (26.7%)	8 (26.7%)	16 (26.7%)	
M1	1 (3.3%)	3 (10.0%)	4 (6.7%)	
M2	5 (16.7%)	6 (20.0%)	11 (18.3%)	
Not reported	16 (53.3%)	13 (43.3%)	29 (48.3%)	

Note: Bold text with "*" represents *p* values with significant difference (*$p<0.05$, **$p<0.01$, ***$p<0.001$).

peritumor tissues showed that the $CD8^+$ T-cell infiltration level in the $P_{extreme}$ group was significantly higher than the P_{stable} group (Figure 3C,D). Because the $P_{extreme}$ group showed significantly worse prognosis (Figure 1E,F), this result pointed out that more $CD8^+$ T cells might be stuck in the peritumor, while failing to infiltrate into the tumor tissue. To confirm this hypothesis, we compare the relative $CD8^+$ T-cell infiltration in tumor, which is defined as the ration of infiltration between tumor and corresponding peritumor. Consistently, the relative $CD8^+$ T-cell infiltration in tumor is significantly lower in the $P_{extreme}$ group (Figure 3E), suggesting that these cytotoxic T cells faced greater difficulty in infiltrating into tumor regions. Altogether, these results suggest that the dysregulation of global circRNA abundance in both tumor and peritumor would obstruct the $CD8^+$ T cells from invading into the tumor.

To identify whether any specific circRNA was involved in the immune infiltration regulation, we further divided the enrolled patients according to the abundance of each circRNA using its mean expression as cutoff. Comparison of immune-infiltration level among different patient groups revealed that only two circRNAs (hsa_circ_0007444 and hsa_circ_0009043) showed their abundance related to $CD8^+$ T-cell infiltration level in tumor tissues ($p = 0.0047$ and $p = 0.046$, respectively; Figure S2). Furthermore, we did not identify any circRNA with its abundance correlated to $CD8^+$ T-cell infiltration level in peritumor tissues. These results suggest that the connection between dysregulation of global circRNA abundance and immune infiltration might present an accumulated effect of all circRNA expression rather than a few certain circRNAs.

Regulatory effect of pre-mRNA spliceosomes on global circRNA abundance

CircRNA has proven to serve as a complementary way for pre-mRNA shearing to protein-coding genes, which means that inhibition or slowing of canonical pre-mRNA processing events could lead to a higher yield of circRNAs.[22] In our analysis, the results of WGCNA in peritumor also indicated the negative relationship between global circRNA abundance and spliceosome pathway (Figure 2D). Meanwhile, comparison between tumor and peritumor samples revealed that most circRNAs were expressed significantly low in HCC (Figure 4A), with most of the spliceosome genes showing opposite trends (Figure 4B), also indicating the potential negative correlation between circRNAs and spliceosome genes. Noteworthily, CRI was confirmed to be negatively correlated with the expression of genes in the spliceosome pathway as well (Figure 4C). To fully validate the regulation role of spliceosome in global circRNA abundance, we first extracted the intersection of spliceosome genes associated with CRI in tumors and peritumors, including NCBP2, PQBP1, SNRPA1, MAGOHB, THOC2, and SRSF1. Then, each of these six genes were knocked down separately in the HCC cell line (SK-Hep-1 cell) using two siRNAs. The results showed that four of them (PQBP1, SNRPA1, MAGOHB, and THOC2) were successfully knocked down with both siRNAs compared with the siRNA control (Figure 4D). The eight knocked-down (two for each of the included four genes) SK-Hep-1 cells were subject to strand-specific and rRNA-depleted RNA-seq, and the CRI was further calculated to investigate the effect of knockdown on global circRNA abundance (Figure 4E). The results showed that CRI significantly increased when the gene expression of these pre-mRNA spliceosomes was reduced, strongly supporting the negative relationship between global circRNA abundance and spliceosome genes. With previous reports revealing the connection between spliceosome and cancer prognosis,[35] our study demonstrated that circRNAs may act as a medium for spliceosome genes to affect tumor progression in HCC.

To further investigate whether global circRNA abundance could affect tumor cells' growth and migration, we performed CCK8 assay and wound-healing assay to evaluate the proliferation and migration ability of HCC cell lines. As we can observe in Figure 4F and Figure S3, proliferation was inhibited in knocked-down cell lines compared with control cell line, proving that circRNA dysregulation

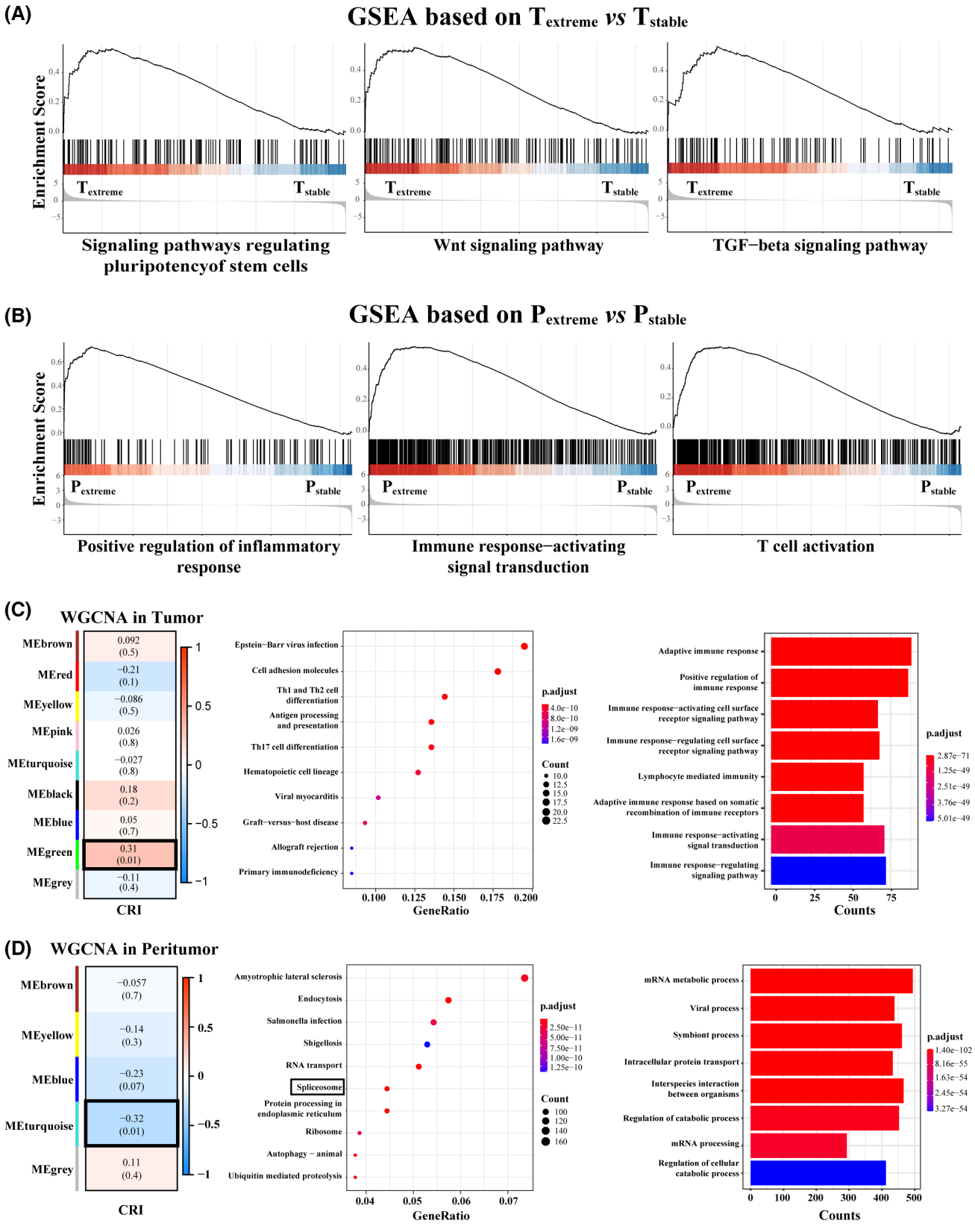

FIGURE 2 Potential regulatory mechanisms underlying overall circRNA abundance. Weighted gene co-expression network analysis (WGCNA) and gene-set enrichment analysis (GSEA) on the tumor and peritumor to explore mechanisms underlying overall circRNA abundance. (A) Pathways associated with tumor growth and immune regulation were significantly enriched in the $T_{extreme}$ group. (B) Pathways associated with immune regulation were significantly enriched in the $P_{extreme}$ group. (C) Genes related with CRI in tumor were enriched in immune regulation pathways. (D) Genes related with CRI in peritumor were enriched in pathways associated with messenger RNA (mRNA) transcription and processing. TGF, transforming growth factor.

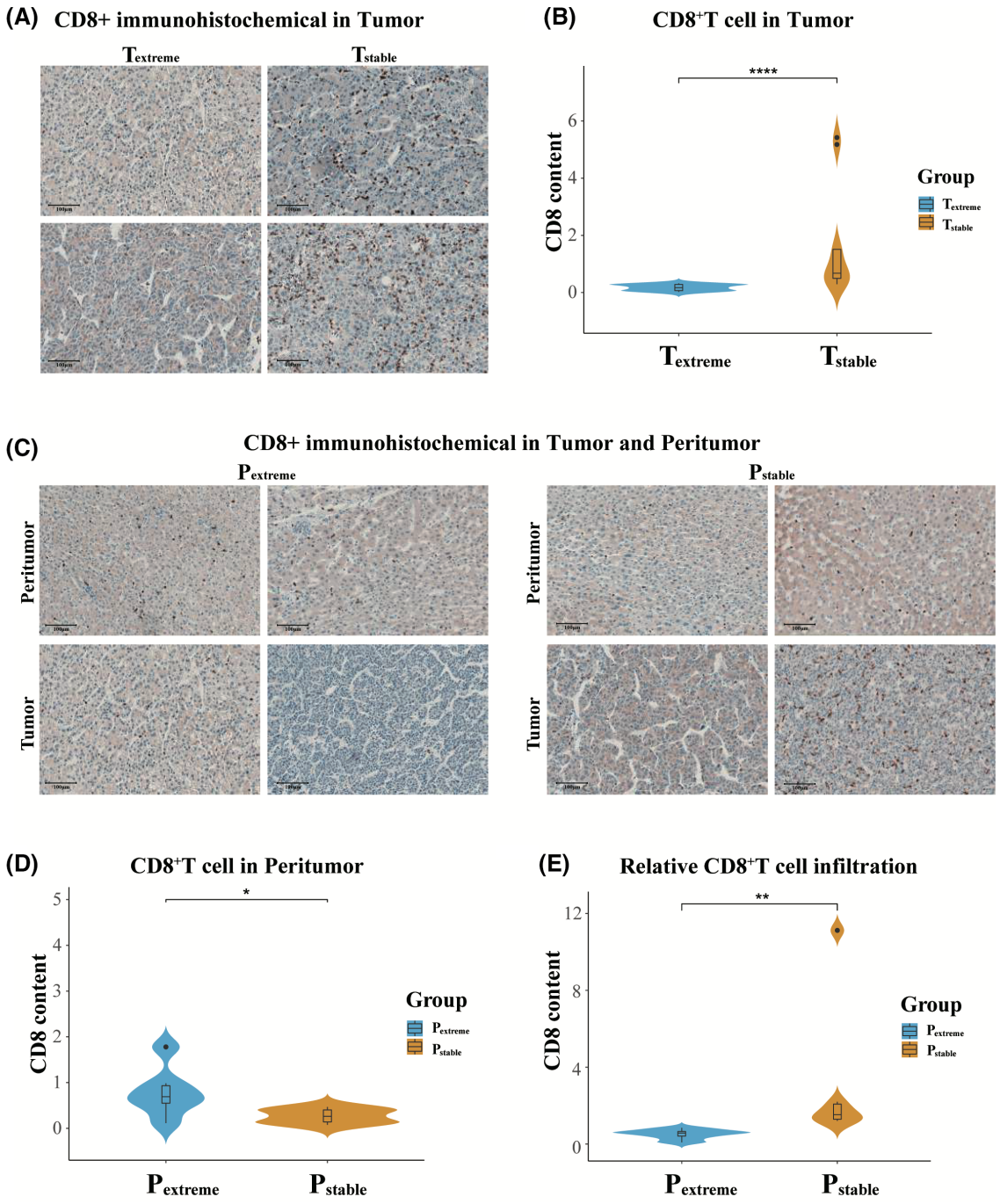

FIGURE 3 Immunohistochemical quantification of $CD8^+$ T cells in tumor and peritumor. (A) $CD8^+$ T cells in tumors; each image represents one sample; the left-hand column is the $T_{extreme}$ group and the right-hand column is the T_{stable} group. (B) Difference analysis of immunohistochemical IHC results between $T_{extreme}$ and T_{stable}. $^{****}p<0.0001$. (C) $CD8^+$ T cells in tumors and matched peritumors; each column represents a pair of samples form 1 patient; the left-hand two columns are the $P_{extreme}$ group and the right-hand two columns are the P_{stable} group. (D,E) Difference analysis of immunohistochemical results between $P_{extreme}$ and P_{stable}. $^{*}p<0.05$, $^{**}p<0.01$.

did affect tumor growth. Meanwhile, the results of wound-healing assay showed that, consistent with the phenomena we observed in CCK8 assays, knockdown of spliceosome genes greatly reduced the cells' capability to migrate (Figure 4G and Figure S4). These experiments validated that circRNA dysregulation played an important role in context with tumor proliferation/migration and helped explain how circRNA overall abundance connected with HCC prognosis.

DISCUSSION

Considering the recognized functional importance and stable characteristics of circRNAs, they have

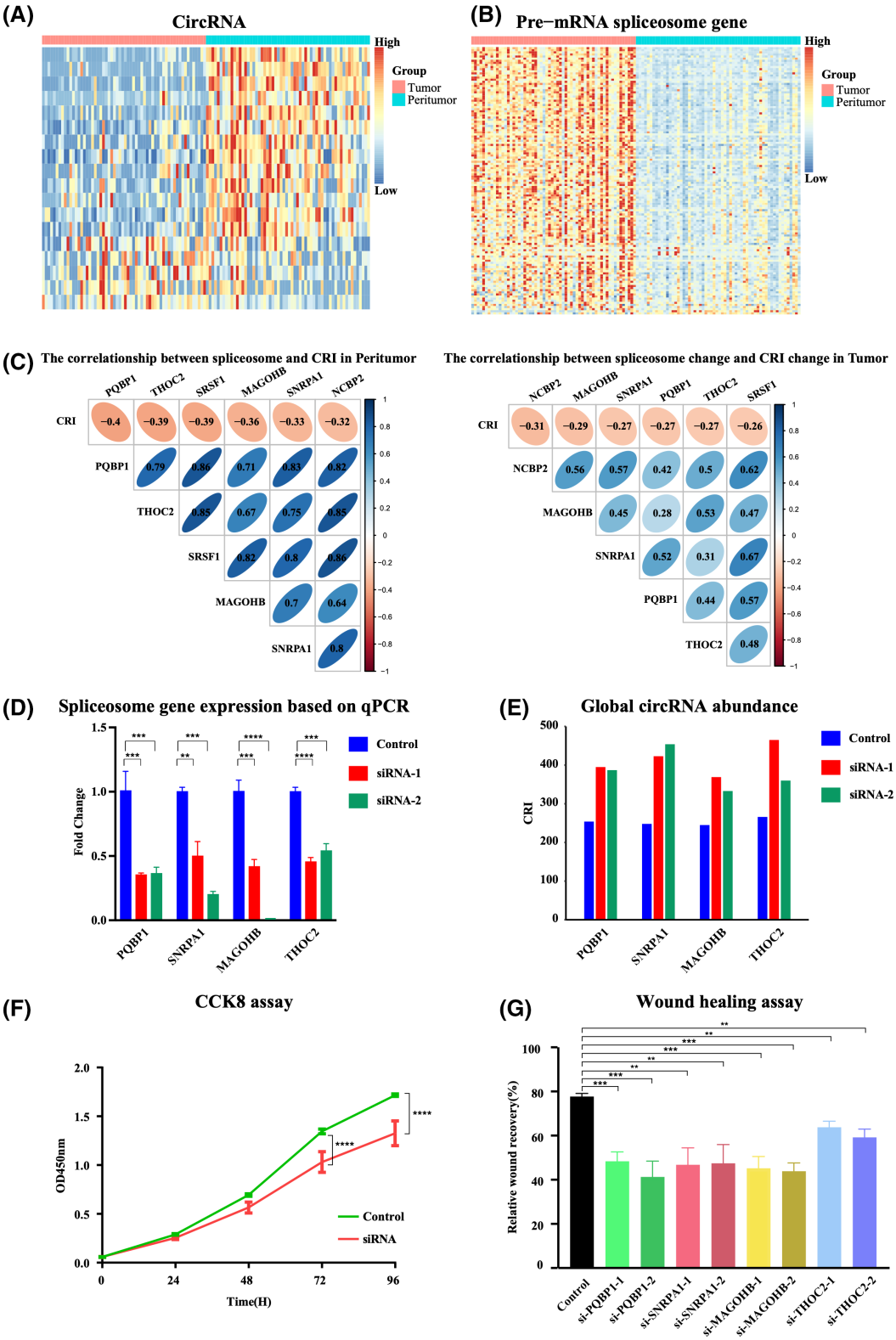

FIGURE 4 Global circRNA abundance is associated with pre-mRNA spliceosome genes. (A) Expression of circRNAs in tumor and matched peritumor; the circRNAs are generally down-regulated in tumors. (B) Expression of pre-mRNA spliceosome genes in tumor and matched peritumor; the spliceosome genes are generally up-regulated in tumors. (C) Relationship between global circRNA abundance and spliceosome genes. (D) Comparison of spliceosome genes between small interfering RNA (siRNA) groups and matched control groups. *$p<0.05$, **$p<0.01$, ***$p<0.001$, ****$p<0.0001$. (E) Comparison of CRI between siRNA groups and matched control groups. (F) Comparison of CCK8 assay between siRNA groups and matched control groups. ****$p<0.0001$. (G) Comparison of wound-healing assay between siRNA groups and matched control groups. **$p<0.01$, ***$p<0.001$. Abbreviation: qPCR, quantitative real-time polymerase chain reaction; PQBP1, Polyglutamine binding protein 1; SRSF1, Serine and arginine rich splicing factor 1; MAGOHB, Mago Homolog B exon junction complex subunit; NCBP2, Nuclear cap binding protein subunit 2; SNRPA1, Small nuclear ribonucleoprotein polypeptide A.

become potential therapeutic targets and biomarkers for HCC. While numerous studies have pointed out the prognostic value of specific circRNAs, use of a single or several circRNAs might not be sufficient to reflect the complicated status of HCC transcriptome, and whether the global expression abundance of circRNA could serve as an indicator for HCC progression remains unknown. In this study, we evaluated the relative global circRNA abundance and found that dysregulation of global circRNA abundance has not only happened in tumor, but also in peritumor, and both could lead to significantly poor HCC prognosis. The evaluation of global circRNA abundance provided an integrated view of the full landscape of circRNA expression, which could provide an angle to understand the circRNA expression dynamics during HCC progression, which could further benefit both diagnosis and prognosis evaluation.

With immune cells serving as the major components for recognizing and killing tumor cells, one major problem in a related field is how tumor and environmental transcriptome feature could affect the interaction between immune system and tumor. In this study, we also found that global circRNA abundance was indeed significantly associated with immune regulatory pathways. Further IHC studies confirmed that global circRNA abundance in tumor tissues was related to $CD8^+$ T-cell infiltration. Surprisingly, despite the significantly higher level of $CD8^+$ T cells in peritumor of the $P_{extreme}$ group, the ratio of $CD8^+$ T cells between tumor and matched peritumor showed significant decrease. These analyses indicated the connection between the circRNA expression status and the immune microenvironment. It is not rare that the circRNAs have a very important impact on the immune system, as pointed out by numerous other studies.[36–38] Our analysis demonstrates that global circRNA abundance could be used to evaluate the overall impact of transcriptome dysregulation and immune infiltration. A further exploration of the detailed mechanism underlining these phenomena is in need to fully understand how circRNA abundance in both tumor and peritumor might take part in the immune regulation.

Previous reports have pointed out the dynamic balance between canonical pre-mRNA processing and circRNA production, which is regulated by pre-mRNA spliceosomes.[22] Consequently, spliceosomes might serve as the most important factors affecting circRNA landscape, with its ability to simultaneously regulate the generation of a large scale of circRNAs at the same time, and thus significantly contribute to the overall abundance of circRNAs. Our analysis has proven that pre-mRNA spliceosomes were indeed the main regulatory factors for circRNA production, suggesting that disordered spliceosome genes contribute to the dysregulation of global circRNA abundance for further promotion of HCC progression. It is not surprising, as spliceosome genes have already been reported with major roles in the tumorigenesis of multiple cancers,[39,40] with their functional importance in transcriptome regulation noteworthily highlighted. Our analyses also indicated an important aspect of their regulation in circRNAs, which might further benefit the better understanding of how these genes were involved in tumor progression. Taken together, these findings indicate that spliceosome genes might be the driving genes for the occurrence and progression of HCC and could be a new target for HCC governance. Analysis of the pre-mRNA process might provide a strategy for monitoring tumor development, benefiting both diagnosis and prognosis evaluation.

In conclusion, our study revealed that the global circRNA abundance in both tumor and matched peritumor was significantly associated with HCC prognosis, showing that circRNA macroscopic expression could play an important role in influencing HCC progression. Furthermore, this influence might be the result of affecting immune cell infiltration, highlighting the potential link between transcriptome landscape and immune system. We also confirmed that the pre-mRNA spliceosomes are the major regulators for the global circRNA abundance in HCC. Taken together, our work indicated the spliceosome-circRNA-immune system axis in the progression of HCC; future investigation is still needed to fully understand the underlying mechanisms.

FUNDING INFORMATION

Supported by the National Natural Science Foundation of China (81802413) and the Scientific Foundation of Fujian Province (2019J01139).

CONFLICT OF INTEREST

Nothing to report.

ORCID

Xiaolong Liu https://orcid.org/0000-0002-3096-4981

REFERENCES

1. Yang JD, Hainaut P, Gores GJ, Amadou A, Plymoth A, Roberts LR. A global view of hepatocellular carcinoma: trends, risk, prevention and management. Nat Rev Gastroenterol Hepatol. 2019;16:589–604.
2. El-Serag HB. Hepatocellular carcinoma. N Engl J Med. 2011;365:1118–27.
3. Shi M, Li ZY, Zhang LM, Wu XY, Xiang SH, Wang YG, et al. Hsa_circ_0007456 regulates the natural killer cell-mediated cytotoxicity toward hepatocellular carcinoma via the miR-6852-3p/ICAM-1 axis. Cell Death Dis. 2021;12:94.
4. Huang G, Liang M, Liu H, Huang J, Li P, Wang C, et al. CircRNA hsa_circRNA_104348 promotes hepatocellular carcinoma progression through modulating miR-187-3p/RTKN2 axis and activating Wnt/β-catenin pathway. Cell Death Dis. 2020;11:1065.
5. Okholm TLH, Sathe S, Park SS, Kamstrup AB, Rasmussen AM, Shankar A, et al. Transcriptome-wide profiles of circular RNA and RNA-binding protein interactions reveal effects on circular RNA biogenesis and cancer pathway expression. Genome Med. 2020;12:112.

6. Liu H, Lan T, Li H, Xu L, Chen X, Liao H, et al. Circular RNA circDLC1 inhibits MMP1-mediated liver cancer progression via interaction with HuR. Theranostics. 2021;11:1396–411.
7. Kong S, Tao M, Shen X, Ju S. Translatable circRNAs and lncRNAs: driving mechanisms and functions of their translation products. Cancer Lett. 2020;483:59–65.
8. Zhang C, Zhang C, Lin J, Wang H. Circular RNA Hsa_Circ_0091579 serves as a diagnostic and prognostic marker for hepatocellular carcinoma. Cell Physiol Biochem. 2018;51:290–300.
9. Vo JN, Cieslik M, Zhang Y, Shukla S, Xiao L, Zhang Y, et al. The landscape of circular RNA in cancer. Cell. 2019;176:869–81.e13.
10. Li Z, Ruan Y, Zhang H, Shen Y, Li T, Xiao B. Tumor-suppressive circular RNAs: Mechanisms underlying their suppression of tumor occurrence and use as therapeutic targets. Cancer Sci. 2019;110:3630–8.
11. Chen S, Huang V, Xu X, Livingstone J, Soares F, Jeon J, et al. Widespread and functional RNA circularization in localized prostate cancer. Cell. 2019;176:831–43.e22.
12. Llovet JM, Zucman-Rossi J, Pikarsky E, Sangro B, Schwartz M, Sherman M, et al. Hepatocellular carcinoma. Nat Rev Dis Primers. 2016;2:16018.
13. Liu Y, Cao X. The origin and function of tumor-associated macrophages. Cell Mol Immunol. 2015;12:1–4.
14. Zhu H, Cao X. NLR members in inflammation-associated carcinogenesis. Cell Mol Immunol. 2017;14:403–5.
15. Makarova-Rusher OV, Medina-Echeverz J, Duffy AG, Greten TF. The yin and yang of evasion and immune activation in HCC. J Hepatol. 2015;62:1420–9.
16. Xiao X, Lao XM, Chen MM, Liu RX, Wei Y, Ouyang FZ, et al. PD-1hi identifies a novel regulatory B-cell population in human hepatoma that promotes disease progression. Cancer Discov. 2016;6:546–59.
17. Chen MM, Xiao X, Lao XM, Wei Y, Liu RX, Zeng QH, et al. Polarization of tissue-resident TFH-like cells in human hepatoma bridges innate monocyte inflammation and M2b macrophage polarization. Cancer Discov. 2016;6:1182–95.
18. Zhou SL, Zhou ZJ, Hu ZQ, Huang XW, Wang Z, Chen EB, et al. Tumor-associated neutrophils recruit macrophages and T-regulatory cells to promote progression of hepatocellular carcinoma and resistance to sorafenib. Gastroenterology. 2016;150:1646–58.e17.
19. Villanueva A. Hepatocellular carcinoma. N Engl J Med. 2019;380:1450–62.
20. Ma S, Kong S, Wang F, Ju S. CircRNAs: biogenesis, functions, and role in drug-resistant tumours. Mol Cancer. 2020;19:119.
21. Zhou WY, Cai ZR, Liu J, Wang DS, Ju HQ, Xu RH. Circular RNA: metabolism, functions and interactions with proteins. Mol Cancer. 2020;19:172.
22. Liang D, Tatomer DC, Luo Z, Wu H, Yang L, Chen LL, et al. The output of protein-coding genes shifts to circular RNAs when the pre-mRNA processing machinery is limiting. Mol Cell. 2017;68:940–54.e3.
23. Wang M, Hou J, Muller-McNicoll M, Chen W, Schuman EM. Long and repeat-rich intronic sequences favor circular RNA formation under conditions of reduced spliceosome activity. iScience. 2019;20:237–47.
24. Harrow J, Denoeud F, Frankish A, Reymond A, Chen CK, Chrast J, et al. GENCODE: producing a reference annotation for ENCODE. Genome Biol. 2006;7(Suppl 1):S4.
25. Dobin A, Davis CA, Schlesinger F, Drenkow J, Zaleski C, Jha S, et al. STAR: ultrafast universal RNA-seq aligner. Bioinformatics. 2013;29:15–21.
26. Li B, Dewey CN. RSEM: accurate transcript quantification from RNA-Seq data with or without a reference genome. BMC Bioinformatics. 2011;12:323.
27. Gao Y, Zhang J, Zhao F. Circular RNA identification based on multiple seed matching. Brief Bioinform. 2018;19:803–10.
28. Ritchie ME, Phipson B, Wu D, Hu Y, Law CW, Shi W, et al. limma powers differential expression analyses for RNA-sequencing and microarray studies. Nucleic Acids Res. 2015;43:e47.
29. Yu G, Wang LG, Han Y, He QY. clusterProfiler: an R package for comparing biological themes among gene clusters. OMICS. 2012;16:284–7.
30. Langfelder P, Horvath S. WGCNA: an R package for weighted correlation network analysis. BMC Bioinformatics. 2008;9:559.
31. Li Y, Tang L, Guo L, Chen C, Gu S, Zhou Y, et al. CXCL13-mediated recruitment of intrahepatic CXCR5(+)CD8(+) T cells favors viral control in chronic HBV infection. J Hepatol. 2020;72:420–30.
32. Zhou Y, Shi WY, He W, Yan ZW, Liu MH, Chen J, et al. FAM122A supports the growth of hepatocellular carcinoma cells and its deletion enhances Doxorubicin-induced cytotoxicity. Exp Cell Res. 2020;387:111714.
33. Xie SC, Zhang JQ, Jiang XL, Hua YY, Xie SW, Qin YA, et al. LncRNA CRNDE facilitates epigenetic suppression of CELF2 and LATS2 to promote proliferation, migration and chemoresistance in hepatocellular carcinoma. Cell Death Dis. 2020;11:676.
34. Burger JA, Wiestner A. Targeting B cell receptor signalling in cancer: preclinical and clinical advances. Nat Rev Cancer. 2018;18:148–67.
35. López-Cánovas JL, del Rio-Moreno M, García-Fernandez H, Jiménez-Vacas JM, Moreno-Montilla MT, Sánchez-Frias ME, et al. Splicing factor SF3B1 is overexpressed and implicated in the aggressiveness and survival of hepatocellular carcinoma. Cancer Lett. 2021;496:72–83.
36. Zhang XL, Xu LL, Wang F. Hsa_circ_0020397 regulates colorectal cancer cell viability, apoptosis and invasion by promoting the expression of the miR-138 targets TERT and PD-L1. Cell Biol Int. 2017;41:1056–64.
37. Jin H, Jin X, Zhang H, Wang W. Circular RNA hsa-circ-0016347 promotes proliferation, invasion and metastasis of osteosarcoma cells. Oncotarget. 2017;8:25571–81.
38. Liu T, Ye P, Ye Y, Lu S, Han B. Circular RNA hsa_circRNA_002178 silencing retards breast cancer progression via microRNA-328-3p-mediated inhibition of COL1A1. J Cell Mol Med. 2020;24:2189–201.
39. Xu W, Huang H, Yu L, Cao L. Meta-analysis of gene expression profiles indicates genes in spliceosome pathway are up-regulated in hepatocellular carcinoma (HCC). Med Oncol. 2015;32:96.
40. Zhang D, Hu Q, Liu X, Ji Y, Chao HP, Liu Y, et al. Intron retention is a hallmark and spliceosome represents a therapeutic vulnerability in aggressive prostate cancer. Nat Commun. 2020;11:2089.

SUPPORTING INFORMATION

Additional supporting information can be found online in the Supporting Information section at the end of this article.

How to cite this article: He L, Qiu L, Chen F, Chen T, Peng F, Li Z, et al. Dysregulation of global circular RNA abundance regulated by spliceosomes predicts prognosis in hepatocellular carcinoma. Hepatol Commun. 2022;6:3578–3591. https://doi.org/10.1002/hep4.2074